

## Polyetheretherketone/Zinc-aluminum 합금 복합체의 열전도율 및 접합본딩 특성에 관한 연구

Y. Peng\*, C. G. Long\*<sup>\*,\*\*,\*†</sup>, X. Peng\*, and Q. C. Liu\*\*\*

\*Institute of Automobile and Mechanical Engineering, Changsha University of Science and Technology

\*\*Key Laboratory of Lightweight and Reliability Technology for Engineering Vehicle, College of Hunan Province

\*\*\*Institute of Physical and Electronic Science, Changsha University of Science and Technology

(2019년 12월 24일 접수, 2020년 3월 4일 수정, 2020년 4월 13일 채택)

## Study on Thermal Conductivity and Interface Bonding Properties of Polyetheretherketone/Zinc-aluminum Alloy Composites

Y. Peng\*, C. G. Long\*<sup>\*,\*\*,\*†</sup>, X. Peng\*, and Q. C. Liu\*\*\*

\*Institute of Automobile and Mechanical Engineering, Changsha University of Science and Technology, Changsha 410114, China

\*\*Key Laboratory of Lightweight and Reliability Technology for Engineering Vehicle,  
College of Hunan Province, Changsha 410114, China

\*\*\*Institute of Physical and Electronic Science, Changsha University of Science and Technology, Changsha 410114, China

(Received December 24, 2019; Revised March 4, 2020; Accepted March 13, 2020)

**Abstract:** In order to improve the thermal conductivity of polyetheretherketone (PEEK), the ZA8 zinc aluminum alloy powder was used as a thermal conductive filler. PEEK / ZA8 thermal composites were prepared by the molding process. The effects of surface modification and ZA8 contents on the thermal conductivity and mechanical properties of PEEK / ZA8 composites were investigated. Meanwhile, the first-principle calculation method based on density functional theory was used to study the surface adsorption characteristics and interface bonding mechanism of the PEEK / ZA8. Results show that the thermal conductivity of the composites is improved after ZA8 surface modification, but the mechanical properties of the composites decreased with the increase of ZA8 content. When the ZA8 content is 40%, the thermal conductivity of the composites is  $0.298 \text{ Wm}^{-1}\text{K}^{-1}$ , which is 72.25% higher than that of pure PEEK. On this basis, 5 wt% graphite is added, the thermal conductivity is  $0.418 \text{ Wm}^{-1}\text{K}^{-1}$ , which is 40.27% higher than that of PEEK / ZA8 without graphite, and 141.62% higher than that of pure PEEK. The first-principle calculation results show that the existence of hydroxyl group can change the adsorption properties of aluminate on Zn (001) surface. From physical adsorption to chemical adsorption, the bond strength between aluminate and Zn surface is greatly improved.

**Keywords:** thermal conductivity, interface bonding mechanism, first-principle, hydroxyl group, aluminate.

### Introduction

In recent years, with the application of polymer materials in automobiles, electronics, aerospace, and heat exchange engineering, the demand for high temperature resistant, corrosion resistant, high-strength thermally conductive composite materials is increasing.<sup>1,2</sup> Therefore, obtaining thermally conductive composite materials with excellent thermal conductivity per-

formance and easy processing has become one of the hot research topics in polymer field.<sup>3</sup> The polymer resin has a low thermal conductivity, and it is difficult to obtain high thermal conductivity by changing its structure, and the cost is high, which is not suitable for industrial production. Therefore, the composite of high thermal conductivity filler and polymer resin matrix becomes an effective method to improve the thermal conductivity of materials.<sup>4-7</sup>

Polyetheretherketone (PEEK) is a high performance semi-crystalline thermoplastic polymer with high glass transition temperature ( $T_g=143 \text{ }^\circ\text{C}$ ) and melting point ( $T_m=343 \text{ }^\circ\text{C}$ ), which can be used at  $250 \text{ }^\circ\text{C}$  for a long time. It has excellent

<sup>†</sup>To whom correspondence should be addressed.  
642426853@qq.com, ORCID<sup>®</sup>0000-0002-1784-7246  
©2021 The Polymer Society of Korea. All rights reserved.

mechanical properties, chemical inertness and good thermal stability over a wide temperature range, making it widely used as a substitute for many metal parts, bearing materials, bone implants and piston rings.<sup>8-10</sup> In recent years, breakthroughs have been made in the research of PEEK-based composites, such as fiber reinforcement, whisker reinforcement and particle filling to improve the friction and thermal properties of PEEK,<sup>11-13</sup> but the preparation of high temperature resistant thermal conductive composites has not attracted enough attention, and there are few relevant reports.<sup>14,15</sup>

China is short of copper resources and rich in zinc ore reserves, which is a superior resource.<sup>16</sup> At present, zinc aluminum alloy, especially high aluminum zinc-based alloy, is one of the most widely used wear-resistant materials.<sup>17</sup> It has the advantages of low friction coefficient, small wear, high thermal conductivity, low melting point, good affinity with lubricating oil and self-lubricating.<sup>18</sup> It has become a substitute for bronze alloy, and is used to make various wear-resistant parts in low speed and heavy load conditions.<sup>19,20</sup> Among all the high aluminum zinc-based alloys, ZA8 zinc aluminum alloy has a low melting point (390 °C), which is close to PEEK melting point and can match it well.

The surface behavior of aluminate coupling agent on inorganic materials often involves the bonding and reaction process at the atomic scale. Therefore, the direct simulation of the interaction between materials from the atomic structure is undoubtedly a more effective way to reveal the modification mechanism of aluminate coupling agent.<sup>21</sup> In recent years, the first-principle calculation has been successfully applied to the study of material microstructure, physical properties and related mechanisms.<sup>22,23</sup> The first-principle calculation is based on quantum mechanics, according to the principle of the interaction between electrons and atoms and the basic law of motion, taking the specific requirements as the starting point, after approximate treatment, the calculation method of solving the Schrodinger equation directly, also known as “ab initio”. This method is mainly used to calculate the structure and basic physical properties of materials. In this paper, ZA8 zinc aluminum alloy is selected as the research model by the first-principle calculation method to study the adsorption characteristics of aluminate coupling agent on the surface of clean and hydroxyl-containing zinc aluminum alloy. And the mechanism of the influence of hydroxyl groups on the adsorption properties of aluminate coupling agent on the surface of zinc aluminum alloy was revealed. The results are expected to provide a theoretical basis for the surface modification of fillers and the

interface design of polymer matrix composites.

In this experiment, the PEEK/ZA8 thermal conductive composite was prepared by molding process with PEEK as the matrix and ZA8 zinc aluminum alloy powders as the thermal conductive filler. The effect of ZA8 powders content on the thermal conductivity and mechanical properties of the composite was studied. The adsorption characteristics of aluminate coupling agent on the surface of clean and hydroxyl-containing zinc aluminum alloy were simulated by the first-principle calculation method.

## Experimental

**Materials.** PEEK was purchased from Jilin Changchun Jida High-tech Materials Co., Ltd, China. ZA8 zinc aluminum alloy powder was supplied by Luxi Antai New Material Technology Co., Ltd, China, 400 mesh. Graphite was provided by Shanghai colloid chemical plant, China, 450 mesh. Aluminate coupling agent was obtained from Foshan Shengyi Plastic Chemical Co., Ltd, China, model DL-411. Sodium hydroxide (NaOH) was obtained from Tianjin Fengchuan Chemical Reagent Technology Co., Ltd, China.

**Hydroxylation Treatment.** According to the action mechanism of aluminate coupling agent, there are physical adsorption and chemical adsorption in the modified filler. Physical adsorption refers to the binding force between aluminate and inorganic filler, which is mainly van der Waals forces and electrostatic force, forming reversible multi-layer adsorption and coating on the surface of inorganic filler. Chemical adsorption refers to the reaction of monoalkoxy group in aluminate coupling agent with hydroxyl hydrogen ion on the surface of filler to form chemical bond (as shown in Figure 1); the other two long organic chains are entangled with polymer molecules<sup>24</sup> (as shown in Figure 2), so as to combine polymer and filler tightly. This process enables the aluminate coupling agent to

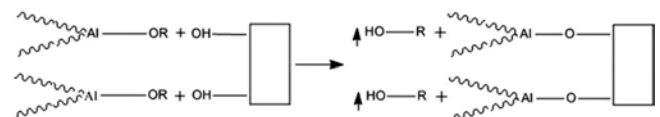


**Figure 1.** Chemical bonding of aluminate and filler.

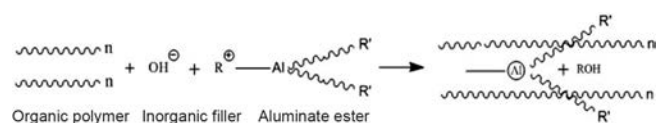


**Figure 2.** Coupling mechanism of aluminate in thermoplastic.

form a single molecular layer on the surface of the filler, which can prevent the viscosity of the filling system from increasing and maintain good fluidity, thus achieving a high filling rate.<sup>25</sup> Therefore, it is necessary to hydroxylate the surface of the filler. The ZA8 powder was mechanically stirred in a 5 mol/L NaOH solution for 12 h to connect a hydroxyl (-OH) functional group to its surface. Then, the particles were washed repeatedly with deionized water to neutrality, and dried to obtain a surface hydroxylated modified ZA8 powder.<sup>26,27</sup>

**Materials Preparation.** The saturated moisture absorption rate of PEEK is about 0.5%. Prior to use, the raw material of PEEK is dried in the oven at 150 °C for 3 h, and then stored in a dryer for standby. Take 1% of the mass of zinc aluminum alloy powder from aluminate coupling agent, put the hydroxylated zinc aluminum alloy into a high-speed mixer (preheat to the material at a temperature of 100-110 °C, Dongguan Muchuan Industrial Co., Ltd, China, model FMD-25) to stir and dry (open) for 10-15 min, so that the water content of zinc aluminum alloy is lower than 0.3%, slowly add a proper amount of comminuted coupling agent, and the blending time was 3-5 min.

The powder of PEEK and ZA8 zinc aluminum alloy were proportioned and evenly mixed, and the composition and distribution are shown in Table 1. The raw materials of each component were ball milled by planetary ball mill (Changsha Deke Instrument Equipment Co., Ltd, China, model DECO-PBM-AD-0.4L), with the processing time of 2 h and the ball material ratio of 10:1. After ball milling, they were taken out for drying.

After cleaning the mold, the high temperature resistant release agent was applied, add the dry mixed powder into the mold, first conduct cold pressing at room temperature, with the loading force of 35 MPa, start to heat up to 390 °C after pressing for 30 min. At the same time, reduce the pressure to 5 MPa, keep the mold at the set temperature for 30 min, then naturally cool the mold to 345 °C, and then increase the pressure to 15 MPa; naturally cool the mold to 80 °C. Next, open the mold and take it out for standby.

**First Principles Calculation.** According to the X-ray diffraction (XRD) curve of ZA8 zinc aluminum alloy (as shown in Figure 3), Zn is the main element in the alloy. Therefore, this paper uses Zn to build the research model. The crystal structure of zinc is a close packed hexagonal structure (hcp), the lattice constant is  $a = b = 0.26649$  nm,  $c = 0.49468$  nm, and the space group is P6/3mm. On the basis of the complete relaxation of zinc crystal, cut (001) crystal surface and add vacuum layer. Considering the calculation workload and periodic boundary conditions, build the surface supercell model of

**Table 1. Proportion of PEEK Based Composite** (unit: wt%)

| Number | 1#  | 2# | 3# | 4# | 5# |
|--------|-----|----|----|----|----|
| ZA8    | 0   | 10 | 20 | 30 | 40 |
| PEEK   | 100 | 90 | 80 | 70 | 60 |

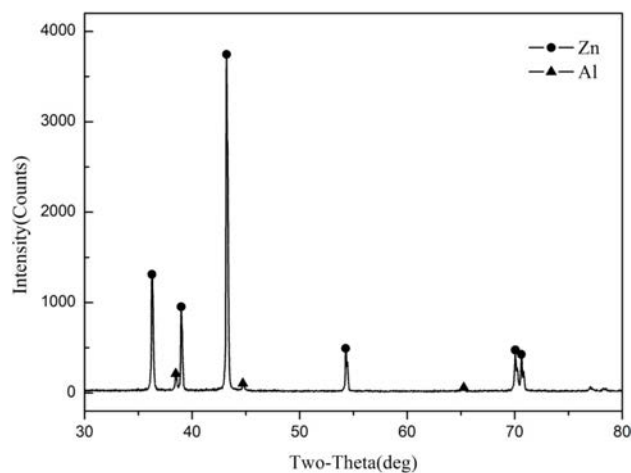


**Figure 3.** The XRD curve of ZA8.

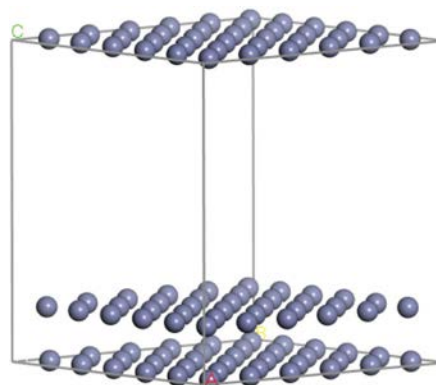


**Figure 4.** The supercell model of Zn (001) surface.

two layers of Zn (001) (6×6). There is interaction between crystal layer and layer. In order to avoid this interference, the thickness of vacuum layer is 10 Å, and the surface model is shown in Figure 4.

The Dmol<sup>3</sup> module based on density functional theory is used in the calculation. When the structure of the model is optimized, the exchange correlation function adopts the PWC form of local density approximation (LDA), the potential function adopts the full electron potential, and the electron wave function adopts the (DNP) basis set. Before the energy calculation, the geometric optimization is carried out to obtain the local stable structure of the model. During the optimization, the accuracy parameters are set as: energy  $\leq 1.0 \times 10^{-5}$  Ha; stress

$\leq 0.002$  Ha; displacement  $\leq 0.005$  Å.

**Performance Test and Characterization.** The surface functional group analysis of hydroxylated ZA8 powder was carried out by Avatar360 Fourier transform infrared spectroscopy (FTIR) (Nicolet Instrument Company, America) and EscaLab 250Xi X-ray photoelectron spectrometer (XPS) (Thermo Fisher Scientific Company, America). FTIR spectra were scanned using radiation in the frequency range 4000–500  $\text{cm}^{-1}$ . In the XPS analysis, a monochromatic Mg  $K\alpha$  X-ray source was used at 1253.6 eV; the Gaussian peak widths were constant in each spectrum during the curve fitting. Scanning electron microscopy (SEM) of MIRA3 (TESCAN Co., Ltd, China) was used to observe the morphology of the ZA8 alloy particles and the cross-section of the samples. The scanning voltage was 20 kV. The thermal conductivity of the composite was tested using a DRL-III thermal conductivity tester (Xiangtan Xiangyi Instrument Co., Ltd, China). The tensile test is carried out on the microcomputer controlled electronic universal testing machine (Shanghai Hualong Test Instrument Co., Ltd, China, model WDW-100C) according to the standard of GB/T 1040.2-2006 with the tensile speed of 2 mm/min; the notched impact strength is carried out on the simple supported beam impact testing machine (Shanghai Hualong Test Instrument Co., Ltd, China, model CBD-7.5) according to the standard of GB/T 1043.1-2008 with the test temperature of 25 °C.

## Results and Discussion

**FTIR and XPS Analysis.** Figure 5 is the FTIR of ZA8 before and after hydroxylation. It can be seen from the spectrum that the absorption peak near 3448  $\text{cm}^{-1}$  corresponds to hydroxyl (-OH). The hydroxyl absorption peak of ZA8 without hydroxylation treatment may be related to the adsorption of water vapor on the surface of the sample. After treatment, the hydroxyl absorption peak of ZA8 is significantly enhanced, which is caused by the numerous free hydroxyl radicals in the alkali solution as electron donor groups. Figure 6 shows the X-ray photoelectron spectroscopy (XPS) of ZA8 after hydroxylation. It can be seen from the chromatogram that there is an obvious O1s peak after sodium hydroxide treatment. Combined with FTIR chromatogram, it can be seen that -OH was successfully grafted on the surface of ZA8 after NaOH solution hydroxylation treatment. According to the modification mechanism of aluminate coupling agent, this will help the aluminate coupling agent to make the aluminate molecules and ZA8 better combine when modifying ZA8.

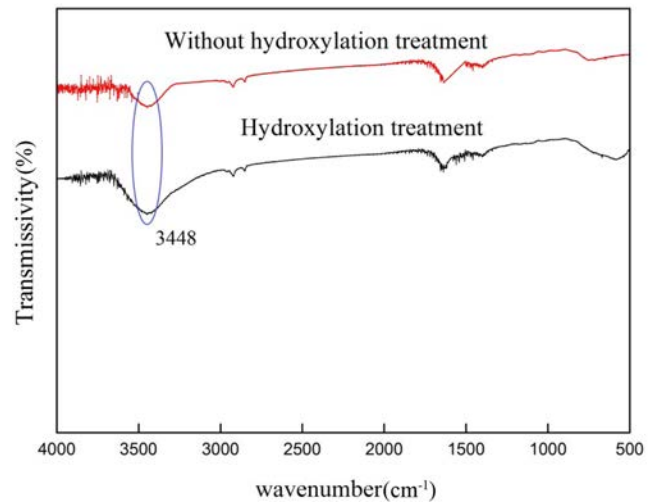


**Figure 5.** FTIR diagram of ZA8 before and after hydroxylation treatment.

**Effect of ZA8 Content on Mechanical Properties before and after Surface Modification.** Figure 7 shows the relationship between the ZA8 content and mechanical properties (tensile strength, tensile modulus, impact strength and elongation) of composites before and after ZA8 surface modification. As shown in the figure, the mechanical properties of ZA8 surface modified composite are better than that of ZA8 unmodified composite. Because in the PEEK/ZA8 composite without surface modification, the basic physical properties of metal powder and resin matrix are slightly different, the compatibility is not good, and the interface bonding strength is not high. In addition, with the increase of ZA8 content, the tensile strength and impact strength of the composite increased first and then decreased gradually. When ZA8 content is 10%, the mechanical properties of the composite are the best, the tensile strength is 111.59 MPa, and the impact strength is 16.21  $\text{kJ/m}^2$ ; With the increase of ZA8 content, both the tensile strength and impact strength of the composite decrease, the toughness of the material decreased, and the fracture was obviously brittle. This is because when the mass fraction of ZA8 is low, the lower matrix damage caused by ZA8 particles and the lower binding energy of the two-phase interface. And the partial effect of aluminate coupling agent makes the mechanical properties of composites decrease less obvious than the pure PEEK, even better than pure PEEK; When too much ZA8 is added, the weak points of particles and polymer matrix increase,<sup>28</sup> and ZA8 limits the movement of PEEK molecular chain, resulting in uneven stress distribution, easy to form stress concentration, resulting in reduced mechanical properties.<sup>29,30</sup>

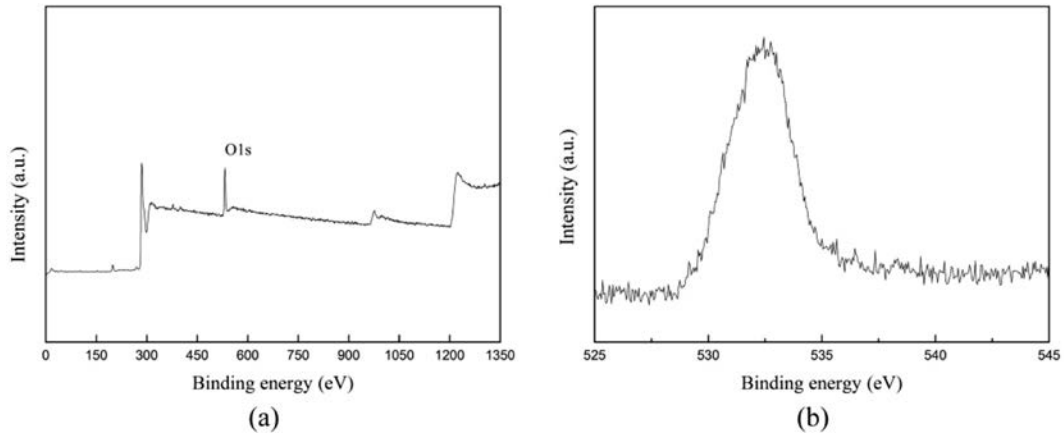


**Figure 6.** XPS analysis of hydroxylated ZA8: (a) XPS survey spectra of ZA8; (b) high-magnification of O1s element of ZA8.

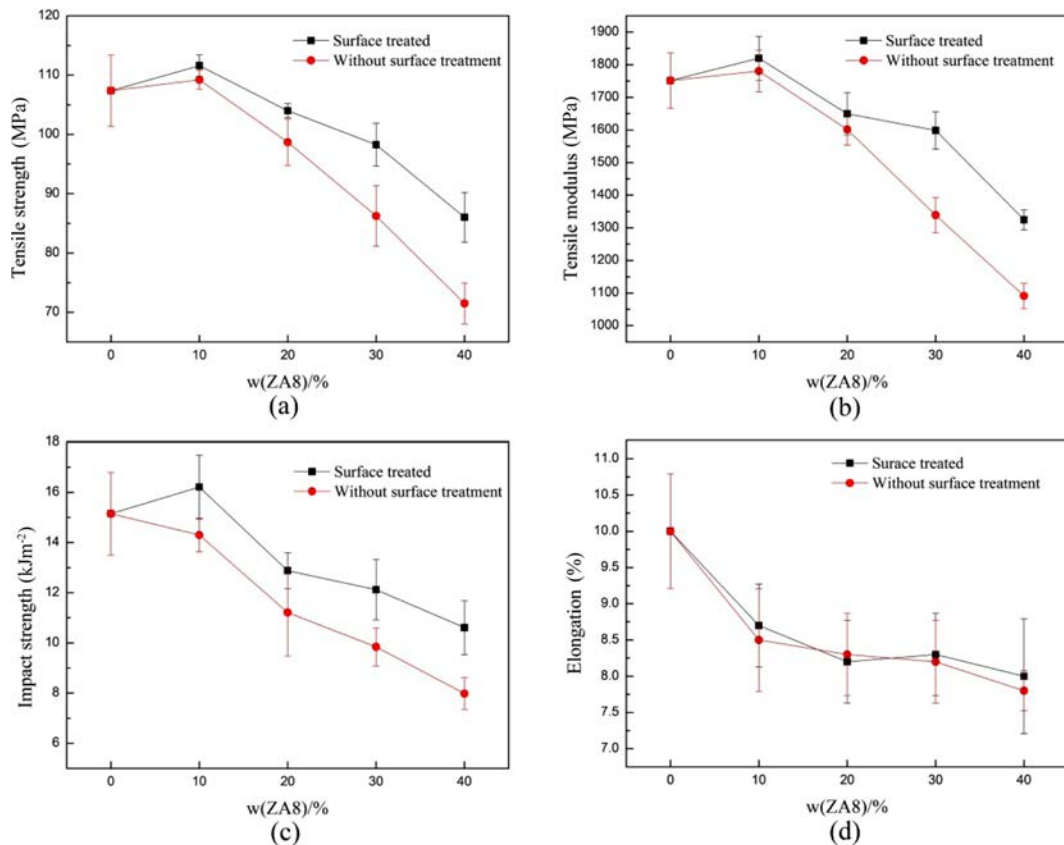


**Figure 7.** Effect of ZA8 content on mechanical properties of composite before and after surface modification: (a) tensile strength; (b) tensile modulus; (c) impact strength; (d) elongation.

**Effect of ZA8 Content on Thermal Conductivity before and after Surface Modification.** Figure 8 shows the relationship between the ZA8 content and thermal conductivity of composite before and after surface modification. In the binary composite system, the heat conduction mainly depends on the effective heat conduction network chain formed by the heat

conduction filler in the matrix resin. So the filler content has an important influence on the heat conduction performance. It can be seen from the figure that the thermal conductivity of the composite increases with the increase of the ZA8 content, and the larger the ZA8 content, the more obvious the growth trend. When the mass fraction of ZA8 is 40%, the thermal con-

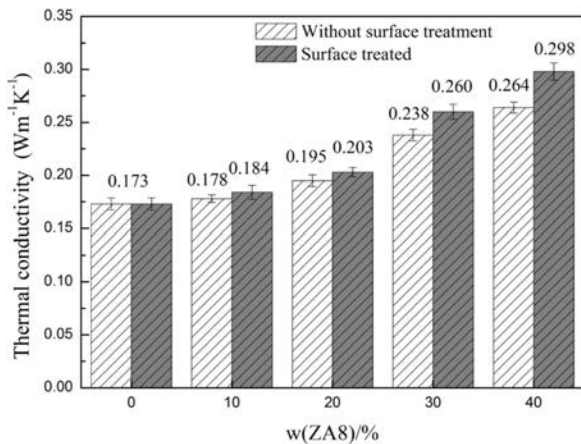


**Figure 8.** Effect of ZA8 content before and after surface modification on thermal conductivity of composites.

ductivity of the composite is  $0.298 \text{ Wm}^{-1}\text{K}^{-1}$ , which is 72.25% higher than that of pure PEEK. This is because when the mass fraction of ZA8 is small, when the fillers form the thermal conductive network chain, the fillers will form a larger space between each other. And it then be filled by the matrix resin with a lower thermal conductivity, resulting in a small improvement in the thermal conductivity of the composite; When the mass fraction of ZA8 is large, the space between the fillers is reduced and the heat conduction is faster. So the thermal conductivity of the composite is improved more obviously.<sup>31</sup> In addition, compared with the thermal conductivity of the composite without surface modification, the thermal conductivity of the composite after surface modification is better. This is due to the better interface bonding performance of the incompatible metal powder and resin under the action of aluminate coupling agent.

In order to further improve the thermal conductivity of the composite, an appropriate amount of graphite (5 wt%) is added on the basis of ZA8 with certain mass fraction and surface modification. The thermal conductivity of the composite is shown in Figure 9. It can be seen from the figure that for composites with different ZA8 mass fraction, the thermal conductivity of the composite with graphite addition is higher than that of the composite without graphite addition. And the thermal conductivity of composites with 40% ZA8 is  $0.418 \text{ Wm}^{-1}\text{K}^{-1}$ , an increase of 40.27% compared to the thermal conductivity of un-added graphite of  $0.298 \text{ Wm}^{-1}\text{K}^{-1}$ , and an increase of 141.62% compared to the thermal conductivity of pure PEEK of  $0.173 \text{ Wm}^{-1}\text{K}^{-1}$ . This is because graphite belongs to a high thermal conductivity filler. The addition of a small amount of graphite not only enriches the internal thermal conductive net-

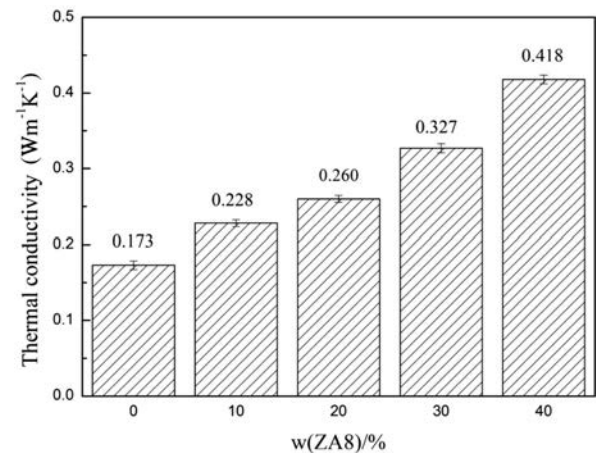


**Figure 9.** Effect of ZA8 on thermal conductivity of 5 wt% graphite composite.

work chain of the composite, but also plays a certain synergistic effect with ZA8,<sup>32,33</sup> so the thermal conductivity of the composite is significantly improved.

**SEM Analysis of PEEK/ZA8 Composite.** Figure 10(a) is the image of ZA8 powder. It can be seen that the zinc aluminum alloy powder particles are generally spherical, with different particle sizes and less than  $20 \mu\text{m}$ . And the particle size proportion is relatively uniform.

Figure 10(b), (c), (d) and (e) are the cross-sectional SEM morphology of pure PEEK, 10% ZA8/PEEK, 20% ZA8/PEEK and 30% ZA8/PEEK composites, respectively. From Figure 9(b), it can be seen that the fracture surface of pure PEEK is smooth and flat, in the form of river. And there is no obvious plastic deformation in the flat area, which is a typical brittle fracture. From Figure 10(c), (d) and (e), it can be seen that the filler is evenly distributed in PEEK resin, and the fracture surface appears a fish scale structure with rich layers, and the fracture surface becomes uneven. The reason for this phenomenon is the addition of ZA8 makes the resin melt adsorbed, and the resin matrix tightly covers the metal particles, which causes the stress concentration, and the rigid particles induce the plastic deformation of the surrounding matrix under the tension. Therefore, the fracture surface is uneven after adding ZA8. With the increase of ZA8 content, the thickness of resin layer between fillers becomes smaller, and because of the small surface area of ZA8 particles, the interface bonding energy between the fillers and the resin matrix decreases. The composite is more vulnerable to damage when subjected to external force. In the process of fracture, ZA8 is completely stripped from the matrix and exposed on the surface.<sup>31</sup> Therefore, the strength of PEEK/ZA8 composite is

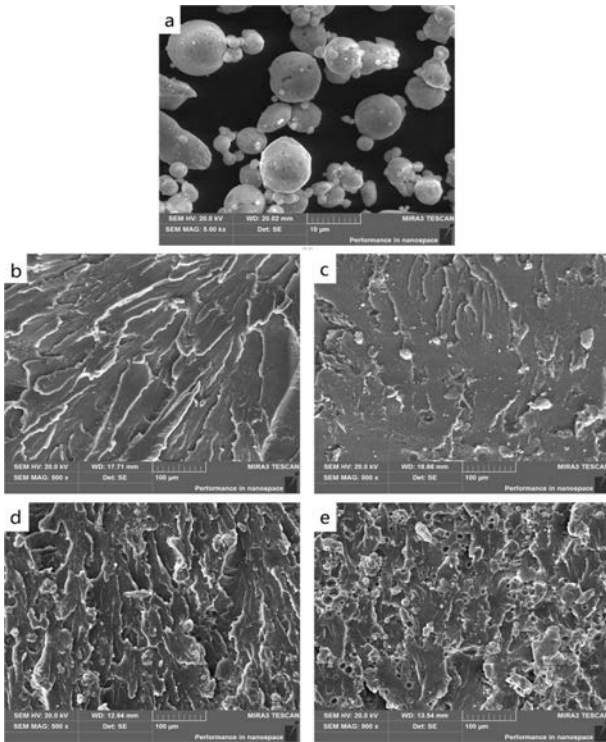


**Figure 10.** Image of ZA8 powder and SEM of cross section: (a) image of ZA8 powder; (b) pure PEEK; (c) 10% ZA8/PEEK; (d) 20% ZA8/PEEK; (e) 30% ZA8/PEEK.

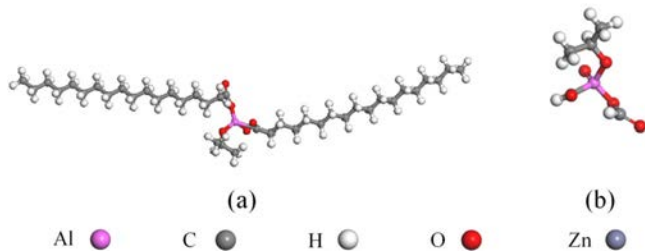


**Figure 11.** Molecular structure of aluminate: (a) molecular structure model of aluminate; (b) simplified molecular structure model of aluminate.

lower than that of pure PEEK, which is consistent with the test of mechanical properties. However, due to the increase of ZA8 content and the decrease of the interaction distance between ZA8 particles, an effective heat conduction chain or network is formed inside the resin matrix, so that the thermal conductivity of the composite is improved.

**Adsorption Characteristics of Aluminate on Clean and Hydroxyl-containing Zn(001) Surface.** The scientific name of DL-411 aluminate coupling agent is isopropylidistearoyl oxyaluminate. Its molecular formula is  $C_{39}H_{77}AlO_5$ , and its molecular weight is 653.01 g/mol. The molecular structure model of aluminate coupling agent is shown in Figure 11(a).

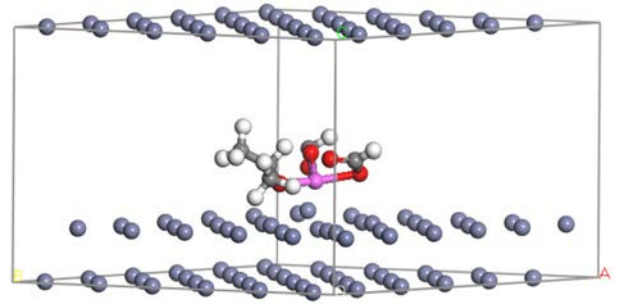


**Figure 12.** Stable adsorption model of aluminate on clean Zn (001) surface.

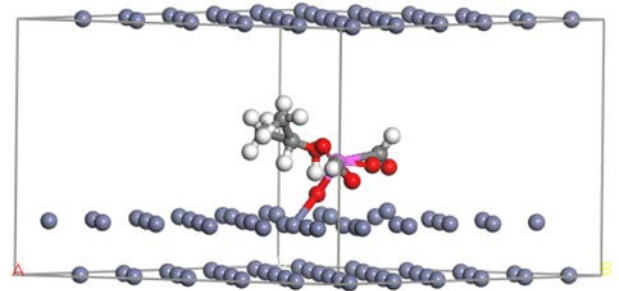


**Figure 13.** Stable adsorption model of aluminate on hydroxyl-containing Zn (001) surface.

Because the molecular structure of aluminate is too large, according to the action mechanism of aluminate coupling agent. The monoalkoxy group in aluminate coupling agent reacts with the hydroxyl hydrogen ion on the surface of filler to form chemical bond. So in order to facilitate calculation, simplify the molecular structure of aluminate, remove the long chain along the both sides, and obtain the simplified molecular structure of aluminate as shown in Figure 11(b).

For the clean Zn (001) system, after relaxation, no bond between the aluminate and the surface atoms of Zn (001) is found (as shown in Figure 12). The aluminate which is very close to the surface of Zn (001) is rejected in the vacuum above the surface after relaxation, indicating that there is no obvious chemical bond between the clean Zn (001) surface and aluminate. The aluminate exhibits physical adsorption properties on the Zn (001) surface.

For the hydroxyl-containing Zn (001) system, after relaxation, the aluminate and Zn (001) surface have obvious chemical bonding (as shown in Figure 13). Including that the Al atom in aluminate and the O atom in the hydroxyl of Zn (001) surface generate bond, while the monoalkoxy group in aluminate also reacts with the hydroxyl hydrogen ion on the surface of Zn (001) to form chemical bond. During the bonding process, the surface hydroxyl plays an “intermediate bridge”

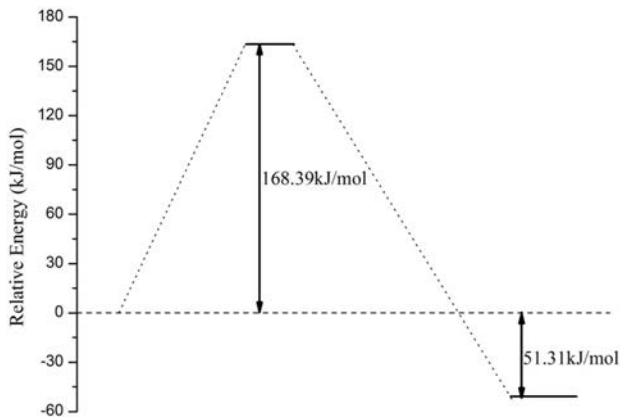


**Figure 14.** Schematic diagram of energy barrier change during covalent bond formation between aluminate and -OH.

role between the aluminate and the Zn surface, which makes the physical adsorption of aluminate on the Zn (001) surface change to chemical adsorption. As the interface adhesion increases, the interface bonding strength between aluminate and Zn (001) surface is significantly improved. This is the reason why the zinc aluminum alloy powder needs to be hydroxylated before surface modification.

According to the chemical bonding theory, the reaction between aluminate and -OH, which includes the process of temperature rising and curing accompanied by the loss of propanol molecules, and the formation of covalent bond with the matrix at the same time. Therefore, the process must provide certain activation energy from the outside.<sup>34</sup> In order to understand the bonding process between aluminate and -OH, the LST/QST method was used to calculate the transition state structure of aluminate combined with -OH, in which taking the stable adsorption structure of aluminate on the surface of Zn (001) containing hydroxyl as the initial state, and the stable adsorption structure of aluminate forming covalent bond with -OH as the final state. As shown in the calculation of Figure 14, the process of forming covalent bond between aluminate and -OH requires a energy barrier of  $E_{\text{bar}} = 168.39$  kJ/mol provided by the outside, and the energy difference before and after the reaction is  $\Delta E = -51.31$  kJ/mol. Under the condition of heating and curing, the activation energy provided by the outside will be far greater than the energy barrier of 168.39 kJ/mol, so the reaction can be carried out completely under the premise of sufficient temperature.<sup>35</sup>

## Conclusions

1) In PEEK/ZA8 composite system, the surface modification

of ZA8 can improve the thermal conductivity and mechanical properties of the composite obviously. When the ZA8 content is 10%, the mechanical properties of the composite reach the best value, the tensile strength is 111.59 MPa, and the impact strength is 16.21 kJ/m<sup>2</sup>.

2) When the content of ZA8 is 40%, the thermal conductivity of PEEK/ZA8 composite is 0.298 Wm<sup>-1</sup>K<sup>-1</sup>, which is 72.25% higher than that of pure PEEK. When 5 wt% graphite is added, the thermal conductivity is further improved to 0.418 Wm<sup>-1</sup>K<sup>-1</sup>, which is 141.62% higher than pure PEEK. Indicating that ZA8 has good synergy with graphite, which significantly improves the thermal conductivity of PEEK.

3) The results of the first-principle calculation show that the existence of hydroxyl group makes the aluminate change from physical adsorption to chemical adsorption on the surface of Zn (001), and enhances the bonding strength between aluminate and zinc aluminum alloy.

**Acknowledgments:** Financial support by the Key Scientific Research Foundation of Education Department of Hunan Province is acknowledged. This study was funded by the Key Scientific Research Foundation of Education Department of Hunan Province (No. 14A011), the International Cooperation Project of Ministry of Science and Technology Foundation (0102013DFG52800) and the Key International and Regional Scientific and Technological Cooperation Project of Hunan Province (2014WK2035).

## References

- Xia, R.; Sun, M.; Yang, B.; Qian, J.; Chen, P.; Cao, M.; Miao, J.; Su, L. Morphology, Thermal and Crystallization Properties of Polyamide-6/Boron (BN) Thermal Conductive Composites. *Polym. Korea* **2018**, 42, 230-241.
- Yoon, Y. S.; Oh, M. H.; Kim, A. Y.; Kim, N. The Development of Thermal Conductive Polymer Composites for Heat Sink. *J. Chem. Chem. Eng.* **2012**, 6, 515-519.
- Kim, S. J.; Hong, C.; Jang, K. S. Theoretical Analysis and Development of Thermally Conductive Polymer Composites. *Polymer* **2019**, 176, 110-117.
- Guo, Z.; Zhao, Q.; Li, C.; Wang, S.; Dong, L.; Hu, G.; Yang, Q.; Xiong, C. A Novel Fluid-filler / Polymer Composite as High-temperature Thermally Conductive and Electrically Insulating Material. *Compos. Sci. Technol.* **2017**, 150, 128-134.
- Goldin, N.; Dodiuk, H.; Lewitus, D. Enhanced Thermal Conductivity of Photopolymerizable Composites Using Surface Modified Hexagonal Boron Nitrid Fillers. *Compos. Sci. Technol.* **2017**, 152, 36-45.
- Kim, K.; Yang, J.; Kim, J. The Study of Multi-walled Carbon



- Nanotube Surface and Matrix Structure for Thermal Conductive Composite Material. *Polym. Korea* **2018**, 42, 776-783.
7. Vu, M. C.; Park, G. D.; Bae, Y. H.; Kim, S. R. Enhanced Thermal Conductivity of Pressure Sensitive Adhesives Using Hybrid Fillers of SiC Microparticle and SiC Nanoparticle Grafted Graphene Oxide. *Polym. Korea* **2016**, 40, 804-812.
  8. Mordina, B.; Tiwari, R. A Comparative Study of Mechanical and Tribological Properties of Poly(ether ether ketone) Composites Filled by Micro- and Nano-Ni and ZrO<sub>2</sub> Fillers. *J. Compos. Mater.* **2013**, 47, 2835-2845.
  9. Kalin, M.; Zalaznik, M.; Novak, S. Wear and Friction Behaviour of Poly-ether-ether-ketone (PEEK) Filled with Graphene, WS<sub>2</sub> and CNT Nanoparticles. *Wear* **2015**, 332-333, 855-862.
  10. Wang, Q.; Wang, Y.; Wang, H.; Fan, N.; Wang, M.; Liu, H.; Yan, F. Comparative Study of the Effects of Nano-sized and Micro-sized CF and PTFE on the Thermal and Tribological Properties of PEEK Composites. *Polym. Adv. Technol.* **2018**, 29, 896-905.
  11. Choy, C. L.; Kwok, K. W.; Leung, W. P.; Lau, F. P. Thermal Conductivity of Poly(ether-ether-ketone) and Its Short-fiber Composites. *Polym. Sci. B Polym. Phys.* **1994**, 32, 1389-1397.
  12. Riviere, L.; Causse, N.; Lonjon, A.; Dantras, E.; Lacabanne, C. Specific Heat Capacity and Thermal Conductivity of PEEK / Ag Nanoparticles Composites Determined by Modulated Temperature Differential Scanning Calorimetry. *Polym. Degrad. Stabil.* **2016**, 127, 98-104.
  13. Wang, H.; Zhang, S.; Wang, G.; Yang, S.; Zhu, Y. Tribological Behaviors of Hierarchical Porous PEEK Composites with Mesoporous Titanium Oxide Whisker. *Wear* **2013**, 297, 736-741.
  14. Zheng, S.; Hua, W.; Ye, X.; Tian, K.; Huang, W.; Jing, H.; Guo, Y.; Tian, X. Anisotropic Thermally Conductive Flexible Polymer Composites Filled with Hexagonal Born Nitride (h-BN) Platelets and Ammine Carbon Nanotubes (CNT-NH<sub>2</sub>): Effects of the Filler Distribution and Orientation. *Composites Part A* **2018**, 108, 402-412.
  15. Shao, L.; Shi, L.; Li, X.; Song, N.; Ding, P. Synergistic Effect of BN and Graphene Nanosheets in 3D Framework on the Enhancement of Thermal Conductive Properties of Polymeric Composites. *Compos. Sci. Technol.* **2016**, 135, 83-91.
  16. Zhou, Z.; Yao, B.; Duan, L.; Qin, L. Production and Anisotropic Compressibility of 304 Stainless Steel Fiber / ZA8 Zinc Alloy Interpenetrating Phase Composites. *J. Alloy. Compd.* **2017**, 727, 146-152.
  17. Shivakumar, N.; Vasu, V.; Narasaiah, N. Processing and Dry Sliding Wear Behavior of Al<sub>2</sub>O<sub>3</sub> Nanoparticles Reinforced ZA-27 Composites. *Mater. Today: Proc.* **2017**, 4, 4006-4012.
  18. Liu, Y.; Li, H.; Jiang, H.; Lu, X. Effects of Heat Treatment on Microstructure and Mechanical Properties of ZA27 Alloy. *Trans. Nonferrous Met. Soc. China* **2013**, 23, 642-649.
  19. Khan, M. M.; Dixit, G. Effects of Test Environment on the Sliding Wear Behavior Cast Iron, Zinc-Aluminium Alloy and Its Composite. *Int. J. Mater. Metall. Eng.* **2016**, 10, 459-468.
  20. Nagavelly, S.; Velagapudi, V.; Narasaiah, N. Mechanical Properties and Dry Sliding Wear Behaviour of Molybdenum Disulphide Reinforced Zinc-Aluminium Alloy Composites. *Trans. Indian. Inst. Met.* **2017**, 70, 2155-2163.
  21. Lin, X.; Niu, C.; Pan, F.; Chen, H.; Wang, X. The Electronic Structures and Ferromagnetism of Fe-doped GaSb: The First-principle Calculation Study. *Physica B* **2017**, 521, 371-375.
  22. Rasukkannu, M.; Velauthapillai, D.; Vajeeston, P. A First-principle Study of the Electronic, Mechanical and Optical Properties of Inorganic Perovskite Cs<sub>2</sub>SnI<sub>6</sub> for Intermediate-band Solar Cells. *Mater. Lett.* **2018**, 218, 233-236.
  23. Fang, Y.; Zhang, J.; Hua, M.; Zhou, D. Modifying Effects and Mechanisms of Graphene on Dehydrogenation Properties of Sodium Borohydride. *J. Mater. Sci.* **2020**, 55, 1959-1972.
  24. Liu, S.; Ma, C.; Cao, W.; Fang, J. Influence of Aluminate Coupling Agent on Low Temperature Rheological Performance of Asphalt Mastic. *Constr. Build. Mater.* **2010**, 24, 650-659.
  25. Huang, Z.; Wang, N.; Zhang, Y.; Hu, H.; Luo, Y. Effect of Mechanical Activation Pretreatment on the Properties of Sugarcane Bagasse / Poly(vinyl chloride) Composites. *Composites Part A* **2012**, 43, 114-120.
  26. Kim, K.; Kim, J. Vertical Filler Alignment of Boron Nitride / Epoxy Composite for Thermal Conductivity Enhancement via External Magnetic Field. *Int. J. Therm. Sci.* **2016**, 100, 29-36.
  27. Kim, K.; Kim, J. Fabrication of Thermally Conductive Composite with Surface Modified Boron Nitride by Epoxy Wetting Method. *Ceram. Int.* **2014**, 40, 5181-5189.
  28. Sun, S.; Qu, M.; Wang, Z.; Zhao, J.; Xu, J.; Wu, L.; Qiao, Z. Study on Preparation and Properties of Thermally Conductive PEEK / Cu / SCF Composites. *Plast. Sci. Technol.* **2015**, 43, 52-55.
  29. Puertolas, J. A.; Castro, M.; Morris, J. A.; Rios, R.; Anson-Casaos, A. Tribological and mechanical properties of graphene nanoplatelet / PEEK composites. *Carbon* **2019**, 141, 107-122.
  30. Sattari, M.; Molazemhosseini, A.; Naimi-Jamal, M. R.; Khavandi, A. Morphology, Nonisothermal Crystallization Behavior and Mechanical Properties of Polypropylene Modified by Ionomers. *Mater. Chem. Phys.* **2014**, 147, 942-953.
  31. Ning, Y.; Sun, S.; Qu, M.; Wu, L.; Qiao, Z.; Wan, C. Effect of Cu Particle Size on the Properties of PEEK / Cu Thermal Conductive Composites. *Plast. Sci. Technol.* **2017**, 45, 25-28.
  32. Li, Z.; Ju, D.; Han, L.; Dong, L. Formation of More Efficient Thermally Conductive Pathways Due to the Synergistic Effect of Boron Nitride and Alumina in Poly(3-hydroxybutyrate). *Thermochim. Acta.* **2017**, 652, 9-16.
  33. Feng, Y.; Han, G.; Wang, B.; Zhou, X.; Ma, J.; Ye, Y.; Liu, C.; Xie, X. Multiple Synergistic Effects of Graphene-based Hybrid and Hexagonal Born Nitride in Enhancing Thermal Conductivity and Flame Retardancy of Epoxy. *Chem. Eng. J.* **2020**, 379, 122402.
  34. Guo, F.; Long, C.; Zhang, J.; Zhang, Z.; Liu, C.; Yu, K. Adsorption and Dissociation of H<sub>2</sub>O on Al(111) Surface by Density Functional Theory Calculation. *Appl. Surf. Sci.* **2015**, 324, 584-589.
  35. Hua, M.; Li, Y.; Long, C.; Li, X. Structure, Electronic and Elastic Properties of Potassium Hexatitanate Crystal from First-principles Calculations. *Physica B* **2012**, 407, 2811-2815.

**Publisher's Note** The Polymer Society of Korea remains neutral with regard to jurisdictional claims in published articles and institutional affiliations.